Analysis of Spherical Monofractal and Multifractal Random Fields with Cosmological Applications

Ravindi Nanayakkara

Supervisor: Associate Professor Andriy Olenko

Co-Supervisor: Professor Philip Broadbridge

La Trobe University, Australia

Fourth Victorian Research Students' Meeting in Probability and Statistics
September 3, 2020

Overview

Introduction to Cosmic Microwave Background data

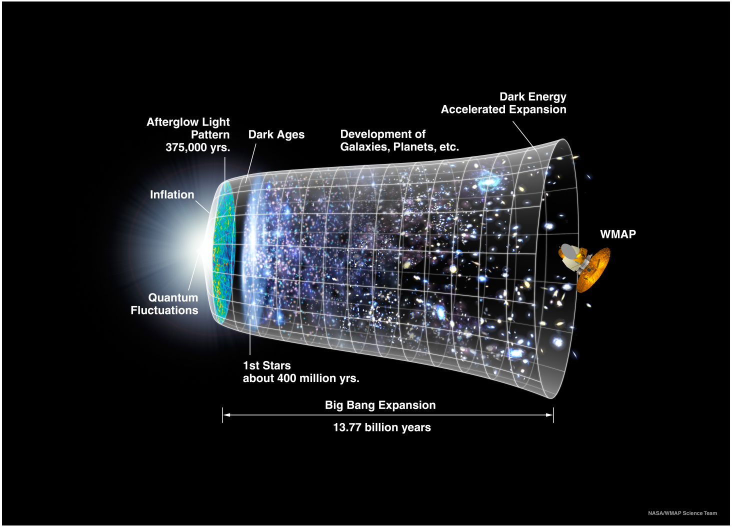

Image credit: NASA / WMAP Science Team

Cosmological Background

- The Cosmic Microwave Background(CMB) is the radiation from the universe since 380,000 years from its birth.
- In Big Bang cosmology, the CMB is an electromagnetic radiation residue from its earliest stage.
- The CMB depicts variations which correspond to different regions and represent the roots for all future formation including the solar system, stars and galaxies in the present world.
- The unforeseen discovery of the CMB was done by Arno Penzias and Robert Wilson who were American radio astronomers.

Cosmological Background

- Earlier, the universe was very hot and dense in nature.
- After the big bang, the universe is expanding and cooling down and had been possible for the atoms to reformulate again after around 400,000 years of its life.
- This phenomenon is known as **Epoch of combination** and since that time photons have been able to move freely escaping from the opaque of the early universe.
- The first light which eliminated from this process is known as the cosmic microwave background.

LA TROBE UNIVERSITY

Missions

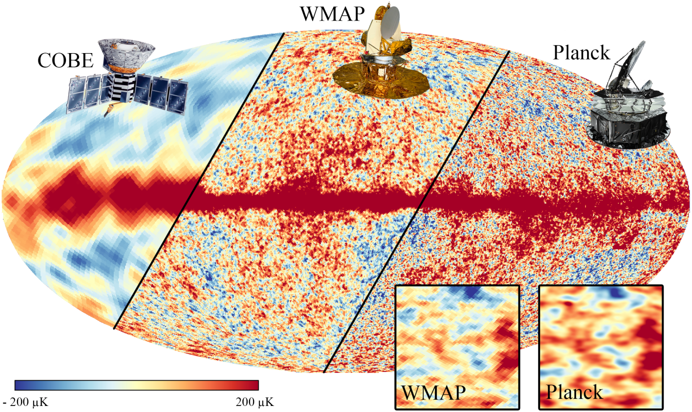

Image credit: https://jgudmunds.wordpress.com

Planck Mission

- In the year 2009, the European Space Agency launched the mission Planck in order to study the CMB thoroughly.
- The frequency range captured by the Planck mission is much wider and its sensitivity is higher than the previous missions of Cosmic Background Explorer(COBE) and Wilkinson Microwave Anisotropy Probe (WMAP).
- Current CMB data are at 5 arc-minutes resolution on the sphere.
- Contains 50,331,648 data collected by Planck mission.

LA TROBE UNIVERSITY

What does CMB data look like?

- Obtained using the newly developed **rcosmo** package.

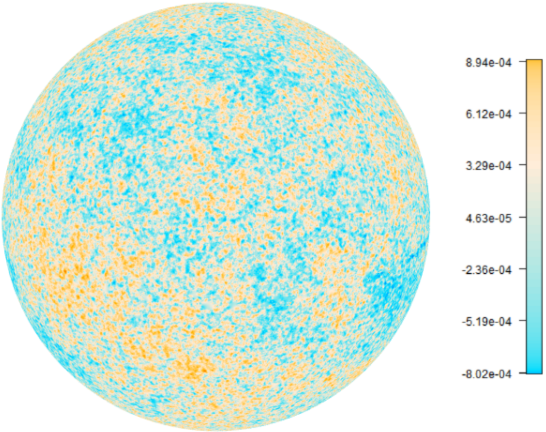

Next Generation Missions

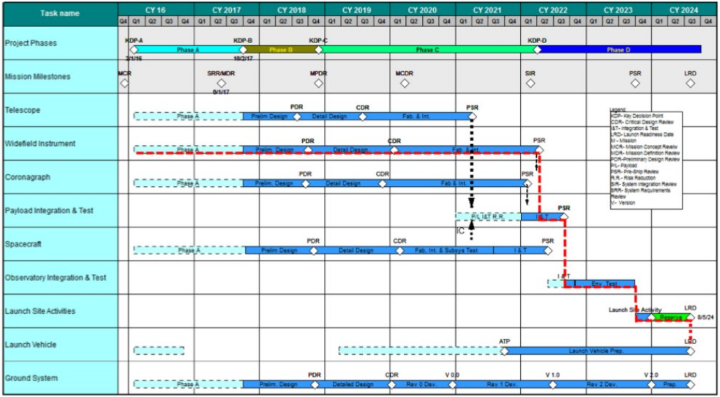

Next Generation Explorer: CMB-S4

(Simons Foundations, NSF and US Department of Energy)

CMB data are available as FITS(Flexible Image Transport System) files stored in HEALPix (Hierarchical Equal Area Isolatitude Pixelation). Each pixel describes distinct location, intensity, polarisation and other CMB attributes.

The HEALPix format has numerous advantages, compared to other spherical data representations:

- equal area pixels,
- hierarchical tessellations of the sphere,
- iso-latitude rings of pixels.

It is used for an efficient organization of spherical data in a computer memory and providing fast spherical harmonic transforms, search and numerical analysis of spherical data.

What does CMB Data Frame look like?

```
> df1<-coords(cmbdf, new.coords = "cartesian")
> df1
A CMBDataFrame
# A tibble: 12,582,912 x 4
       x     y        z           I
   <dbl> <dbl>    <dbl>       <dbl>
 1 0.707 0.707 0.000651 -0.0000920
 2 0.707 0.708 0.00130  -0.0000804
 3 0.708 0.707 0.00130  -0.0000899
 4 0.707 0.707 0.00195  -0.0000771
 5 0.706 0.708 0.00195  -0.0000701
 6 0.705 0.709 0.00260  -0.0000606
 7 0.707 0.708 0.00260  -0.0000663
 8 0.706 0.708 0.00326  -0.0000569
 9 0.708 0.706 0.00195  -0.0000872
10 0.708 0.707 0.00260  -0.0000728
# ... with 12,582,902 more rows
```

Figure: Cartesian Coordinates View

```
> df2<-coords(cmbdf, new.coords = "spherical")
> df2
A CMBDataFrame
# A tibble: 12,582,912 x 3
   theta   phi           I
   <dbl> <dbl>       <dbl>
 1  1.57 0.785 -0.0000920
 2  1.57 0.786 -0.0000804
 3  1.57 0.785 -0.0000899
 4  1.57 0.785 -0.0000771
 5  1.57 0.787 -0.0000701
 6  1.57 0.788 -0.0000606
 7  1.57 0.786 -0.0000663
 8  1.57 0.787 -0.0000569
 9  1.57 0.784 -0.0000872
10  1.57 0.785 -0.0000728
# ... with 12,582,902 more rows
```

Figure: Spherical Coordinates View

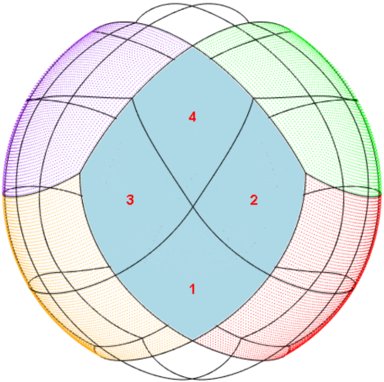

(a) HEALPix nested ordering

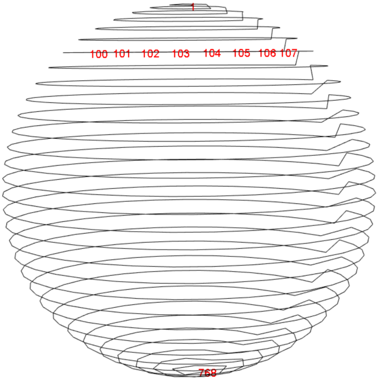

(b) HEALPix ring ordering

Random Fields on a Sphere

- The spherical surface in $\mathbb{R}^3$ (as a two-dimensional mainfold) with a given radius $r > 0$ is

$$s(r) = \{x \in \mathbb{R}^3 : \|x\| = r\}$$

- **Statistical model:** CMB can be viewed as a single realization of a random field on a sphere.

- A spherical random field denoted by, $\xi = \{\xi(r, \theta, \varphi) : 0 \leq \theta \leq \pi, 0 \leq \varphi \leq 2\pi, r > 0\}$ is a stochastic function defined on the sphere $s(r)$.

- We consider a real-valued spherical field such that its covariance function depends on the geodesic (or angular) distance between the two points on the sphere.

Random Fields on a Sphere

Definition 1

A random field $\xi(x), x \in T$ where $T \subseteq \mathbb{R}^n$ is called Gaussian if for any $x^{(1)}, ..., x^{(r)} \in T$, the joint distribution of random variables $(\xi(x^{(1)}), ..., \xi(x^{(r)}))'$ are Gaussian.

Definition 2

A real random field $\xi(u), u \in s(1)$ with $E[\xi^2(u)] < \infty$ and $E[\xi(u)] = 0$ is called isotropic on a sphere if,

$$E[\xi(u)\xi(v)] = B(\cos\theta),$$

$u, v \in s(1)$, depends only on the geodesic (angular) distance $\cos\theta$ between u and v.

LA TROBE UNIVERSITY

Random Fields on a Sphere

- We get the following representation of covariance functions of the isotropic random field on the sphere.

$$B(\cos\theta) = \frac{1}{|s(1)|}\sum_{m=0}^{\infty} b_m h(m,n)\frac{C_m^v(\cos\theta)}{C_m^v(1)}, \tag{1}$$

  where $C_m^v, m = 0, 1, \ldots$ are the Gegenbauer polynomials.

- The representation for $B(\cos\theta)$ implies the spectral decomposition of the isotropic field on the sphere $\xi(u), u \in s(1)$, itself. That is, there exists a real-valued sequence of random variables η_m^l such that

$$\xi(u) = \sum_{m=0}^{\infty}\sum_{l=1}^{h(m,n)} S_m^l(u)\eta_m^l, \tag{2}$$

  where S_m^l are spherical harmonics, and

$$E[\eta_m^l] = 0, \qquad E[\eta_m^l \eta_p^q] = b_m \delta_m^p \delta_l^q.$$

Multifractality

- The concept of multifractality initially emerged in the context of measures where B. Mandelbrot showed the significance of scaling relations in the setting of turbulence modelling.
- A multifractal pattern is a type of a fractal pattern that scales with multiple scaling rules in contrast to monofractals that have only scaling rule and it is a fractal scheme where its dynamics cannot be explained by a single fractal dimension.
- Rényi function which is also known as the deterministic partition function plays a key role in multifractal analysis.
- Leonenko and Shieh (2013) computed the Rényi function for three models of the multifractal random fields and showed some major schemes for the Rényi function that reveal the multifractality of homogeneous and isotropic data.

Definition 3

A stochastic process $\{X(t)\}$ is said to be multifractal if

$$\{X(ct)\} \stackrel{d}{=} \{M(c)X(t)\}, \tag{3}$$

where for every $c > 0$, $M(c)$ is a random variable independent of $\{X(t)\}$ whose distribution does not depend on t.

Definition 4

A stochastic process $\{X(t)\}$ is said to be multifractal if there exist functions $c(q)$ and $\tau(q)$ such that for all $t, s \in \tau, \forall q \in \mathcal{Q}$,

$$E|X(t) - X(s)|^q = c(q)|t - s|^{\tau(q)}. \tag{4}$$

where $\mathcal{T}$ and $\mathcal{Q}$ are intervals on the real line with positive length and $0 \in \mathcal{T}$.

- We consider a real-valued spherical field T with the mean m, and finite second moments such that it is continuous in the mean-square sense and its covariance function depends on the geodesic (or angular) distance between the two points on the sphere.
- Under these conditions, the isotropic random field on the sphere $s_2(r)$ can be expanded in mean-square sense as a Laplace series

$$T(r,\theta,\varphi) = m + \sum_{l=0}^{\infty} \sum_{m=-l}^{l} Y_l^m(\theta,\varphi) a_l^m(r), \tag{5}$$

where $Y_l^m(\theta,\varphi)$ represent the spherical harmonics, i.e.

$$Y_l^m(\theta,\varphi) = c_l^m \exp(im\varphi) P_l^m(\cos\theta),\ -l \le m \le l,\ l = 0,1,\ldots, \tag{6}$$

where

$$c_l^m = (-1)^m \left[\frac{2l+1}{4\pi} \frac{(l-m)!}{(l+m)!}\right]^{1/2},\ -l \le m \le l$$

and $P_l^m(\cos\theta)$ denotes the associated Legendre polynomials of degree l and order m.

- We introduce the following conditions for the spherical random fields on $\mathbb{R}^3$:

Definition 5

(Condition $A^{''}$)
Let the random field $\Lambda = \{\tilde{\Lambda}(x), x \in s_2(1)\}$ be an isotropic random field such that

$$E\tilde{\Lambda}(x) = 1, \quad Var\tilde{\Lambda}(x) = \sigma_\Lambda^2 < \infty, \quad \Lambda(x) > 0, \quad x \in s_2(1),$$

$$Cov(\Lambda(\theta, \varphi), \Lambda(\theta^{'}, \varphi^{'})) = \frac{1}{4}\sum_{l=1}^{\infty}(2l+1)C_l P_l(\cos\theta), \quad \sum_{l=1}^{\infty}(2l+1)C_l < \infty,$$

and $\tilde{\Lambda}^{(i)}(x), x \in s_2(1), i = 0, 1, 2, ...,$ be a sequence of independent fields such that $\tilde{\Lambda}^{(i)}(x) \stackrel{d}{=} \tilde{\Lambda}^{(i)}(b^i x)$, where $b > 1$ is a scaling factor, and we interpret $b^i x$ by $b^i x := (1, b^i \underset{\pi}{\times} \theta, b^i \underset{2\pi}{\times} \varphi) \in s_2(1)$, where the modulus algebra is used accordingly.

- Define the finite product fields on $s_2(1)$

$$\tilde{\Lambda}_k(x) = \prod_{i=0}^{k} \tilde{\Lambda}^{(i)}(b^i x),$$

and the random measure on Borel σ-algebra $\mathcal{B}$ of $s_2(1)$

$$\mu_k(B) = \int_B \Lambda_k(y)dy,\ k = 0, 1, 2, ...,\ B \in \mathcal{B}. \tag{7}$$

- We denote by $\mu_k \xrightarrow{D} \mu,\ k \to \infty$, the weak convergence of the measures μ_k to some non-degenerate measure μ, that is

$$\int_{s_2(1)} f(y)\mu_k(dy) \to \int_{s_2(1)} f(y)\mu(dy),\ k \to \infty,$$

for all continuous functions $f(y), y \in s_2(1)$.

LA TROBE UNIVERSITY

The Rényi function

- The Rényi function of μ on $s_2(1)$ can be defined as

$$T(q) = \liminf_{m\to\infty} \frac{\log_2 E \sum_l \mu(S_l^{(m)})^q}{log_2|S_l^{(m)}|}, \tag{8}$$

  where $\{S_l^{(m)}, l, m\}$, $l = 0, 1, ..., 2^m - 1$ and $m = 1, 2, ...$, is the mesh formed by the mth level dyadic decomposition of the spherical surface $s_2(1)$.

- For the CMB data analysis, we use $\mu(S_l^m)$ which equals the cumulative CMB intensity over S_l^m.

- The statistical estimator $\widehat{T(q)}$ is obtained using the equation (8) and for large values of m.

LA TROBE UNIVERSITY

Assumption 1

(i) *Assume that the correlation function $\rho_\Lambda(\|x-y\|) = \rho(r)$ of a mother field Λ satisfies the following conditions:*

$$\rho_\Lambda(r) \leq Ce^{-\gamma r},\ r > 0, \tag{9}$$

for some positive C and γ. Then, when the scaling factor $b : b > \sqrt[n]{1+\sigma_\Lambda^2}$, on $s_2(1)$, the measures $\mu_k \xrightarrow{D} \mu,\ k \to \infty$. Then the random measure μ is non-degenerate and it has the finite second moment: $E\mu^2(s_2(1)) < \infty$. And also it has the stochastic scaling-invariant (or say self-similar) property $\mu(dy) = b^{-n}\Lambda(y)\hat{\mu}(bdy)$, where the measure $\hat{\mu}(dy)$ is independent of Λ and has the same distribution as $\mu(dy)$.

(ii) *Assume that for some range $q \in Q = [q_-, q_+]$, both $E^q\Lambda(0) < \infty$ and $E\mu^q(s_2(1)) < \infty$.*

UNIVERSITY

Theorem 1

Suppose that the condition A'' holds and the isotropic random field is the restriction of the HIRF $\Lambda(x), x \in \mathbb{R}^3$ with correlation function $\rho_\Lambda(\|x-y\|) = \rho(r)$ on the sphere $s_2(1)$. We assume the above given assumptions.

The Rényi function $T(q)$ of the limit measure μ on $s_2(1)$ is given by

$$T(q) = q - 1 - \frac{1}{2}\log_b E\Lambda^q(t), \quad q \in Q.$$

The multifractal or singularity spectrum is defined via the Legendre transform as

$$f(h) = \inf_q (hq - T(q)). \tag{10}$$

and is used to describe local fractal dimensions of random fields.

Known results about the Rényi function

Model 1: Log-Normal Scenario

$$T(q) = q\left(1 + \frac{\sigma_Y^2}{4\ln b}\right) - q^2\left(\frac{\sigma_Y^2}{4\ln b}\right) - 1, \quad q \in [1,2].$$

Model 2: Log-Gamma Scenario

$$T(q) = q\left(1 - \frac{\beta}{2}\log_b\left(1 - \frac{1}{\lambda}\right)\right) + \left(\frac{\beta}{2}\right)\log_b\left(1 - \frac{q}{\lambda}\right) - 1.$$

where $q \in Q = \{0 < q < \lambda\} \cap [1,2] \cap L_{\beta,\lambda}$.

Model 3: Log-Negative-Inverted-Gamma Scenario

$$T(q) = q\left(1 + \frac{c_U}{2\ln b}\right) - \frac{1}{2}\log_b\left(q^{\beta/2}K_\beta(2\sqrt{q\lambda})\right) - \left(1 + \frac{1}{2}\log_b\left(\frac{2\lambda^{\beta/2}}{\Gamma(\beta)}\right)\right),$$

where $q \in Q = [1,2] \cap L_{\beta,\lambda}$, $K_\lambda(x)$ is the modified Bessel function of the third kind.

LA TROBE UNIVERSITY

Models based on power transformations of Gaussian fields

Model 4:

$$T(q) = q - 1 - \frac{1}{2}\log_b\left(\frac{2^q\Gamma(q+\frac{1}{2})}{\sqrt{\pi}}\right),\ q \in [1,2].$$

Model 5:

$$T(q) = q - 1 - \frac{1}{2}\log_b EY^{2kq}(x) = q - 1 - \frac{1}{2}\log_b\left(\frac{2^{kq}\Gamma(kq+\frac{1}{2})}{\sqrt{\pi}}\right).$$

Model 6:

$$T(q) = q - 1 - \frac{1}{2}\log_b\left(\left(\frac{2}{k}\right)^q EY^q(x)\right) = q\left(1 - \frac{1}{2}\log_b\left(\frac{2}{k}\right)\right) - 1$$

$$-\frac{1}{2}\log_b\left(2^q\frac{\Gamma(q+\frac{k}{2})}{\Gamma(\frac{k}{2})}\right).$$

Computing multifractal spectra for the models

Let $\alpha(q)$ denote the q^{th} order singularity exponent and be defined by

$$\alpha(q) = \frac{d}{dq} T(q).$$

Then the multifractal spectrum defined by (10) can be expressed as a function of α by

$$f(\alpha(q)) = q \cdot \alpha(q) - T(q).$$

Multifractal spectra for model 1:

$$f(\alpha(q)) = 1 - \frac{\sigma_Y^2}{4\ln(b)} q^2, \quad q \in [1, 2].$$

Multifractal spectra for model 2:

$$f(\alpha(q)) = 1 + \frac{\beta}{2}\left(\frac{q}{\ln(b)(q-\lambda)} - \log_b\left(1 - \frac{q}{\lambda}\right)\right).$$

Computing multifractal spectra for the models

Multifractal spectra for model 3:

$$f(\alpha(q)) = 1 + \frac{\beta}{2}\log_b\left(\frac{2\lambda^{\beta/2}}{\Gamma(\beta)}\right) - \frac{\beta}{4\ln(b)} + \frac{1}{2}\log_b(q^{\beta/2}K_\beta(2\sqrt{q\lambda})) + \frac{\sqrt{q\lambda}(K_{\beta-1}(2\sqrt{q\lambda}) + K_{\beta+1}(2\sqrt{q\lambda}))}{2\ln(b)K_\beta(2\sqrt{q\lambda})}.$$

Multifractal spectra for model 4:

$$f(\alpha(q)) = 1 + \frac{1}{2}\log_b\left(\frac{\Gamma(q+\frac{1}{2})}{\sqrt{\pi}}\right) - \frac{q\psi(q+\frac{1}{2})}{2\ln 2}$$

Multifractal spectra for model 5:

$$f(\alpha(q)) = 1 + \frac{1}{2}\log_b\left(\frac{\Gamma(kq+\frac{1}{2})}{\sqrt{\pi}}\right) - \frac{kq\psi(kq+\frac{1}{2})}{2\ln 2}$$

Multifractal spectra for model 6:

$$f(\alpha(q)) = 1 + \frac{1}{2}\log_b\left(\frac{\Gamma(q+\frac{k}{2})}{\Gamma(\frac{k}{2})}\right) - \frac{q\psi(q+\frac{k}{2})}{2\ln 2}.$$

LA TROBE UNIVERSITY

Dependence of the Rényi function on the parameter b

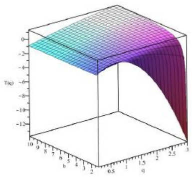

(a) Rényi functions of Model 1

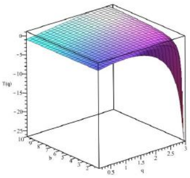

(b) Rényi functions of Model 2

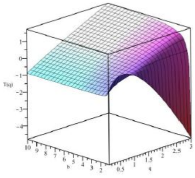

(c) Rényi functions of Model 3

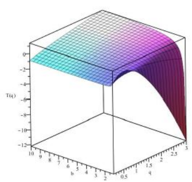

(d) Rényi functions of Model 4

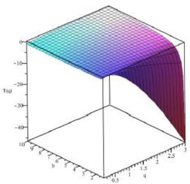

(e) Rényi functions of Model 5

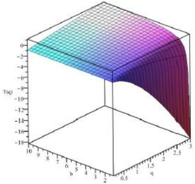

(f) Rényi functions of Model 6

Figure: Dependence of the Rényi function on the parameter b

Simulation methodology

- There are numerous models for which explicit expressions for the Rényi function in terms of elementary functions or even series are not available.
- For such difficult cases, random field simulations can be used to obtain realizations of random fields from theoretical models and compute empirical Rényi functions.
- Figure below shows a realization of a multifractal random field in a large spherical window and this field was obtained from a Gaussian mother random field $Y(x)$ with the exponential covariance model and its variance equals 2.

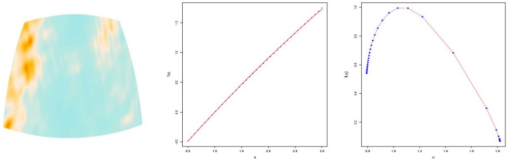

(a) Realization of a multifractal random field (b) Sample Rényi function with the fitted Log-Normal model (c) $f(\alpha)$ versus α

Figure: Realization of a multifractal random field

Computing the Rényi function for CMB data

- Empirical Rényi functions were calculated for real cosmological data obtained from the NASA/IPAC Infrared Science Archive.
- Extensive numerical studies were conducted for different windows in various sky locations.

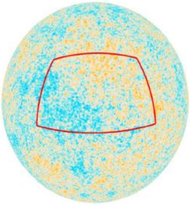

(a) Large window

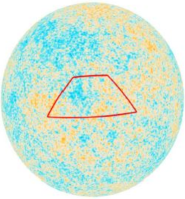

(b) Medium window

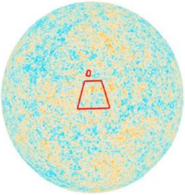

(c) Small and very small windows

Figure: Different sky windows of CMB data

Computing the Rényi function for CMB data

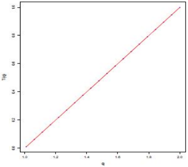

(a) Sample Rényi function versus linear function

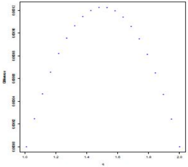

(b) Difference of sample Rényi function and linear function

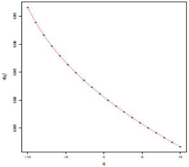

(c) $\alpha(q)$ versus q

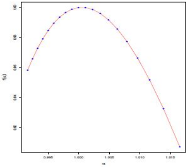

(d) $f(\alpha)$ versus α

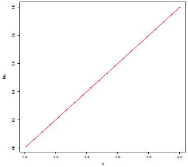

(e) Sample Rényi function with the fitted Log-Normal model

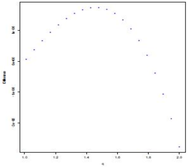

(f) Difference between sample Rényi function and the fitted Log-Normal model

Figure: Whole sky data analysis

LA TROBE UNIVERSITY

Computing the Rényi function for CMB data

- First the Rényi function was computed for the whole sky.
- It is clear from the analysis that the departure from a linear behaviour is not substantial.
- All these plots confirm only very small multifractality of the CMB data.
- The Rényi functions, multifractal spectra, similar analysis and plots were produced for different window sizes of the CMB unit sphere.
- Large, medium, small and very small window sizes with areas 1.231, 0.4056, 0.0596 and 0.0017 were selected.
- The Rényi function was computed for small windows located at different places of the sky sphere such as near the pole, near the equator and other places of the sphere.
- Although different window sizes of the sphere were investigated, there's not that much of evidence to suggest that we have substantial multifractality.

LA TROBE UNIVERSITY

Computing the Rényi function for CMB data

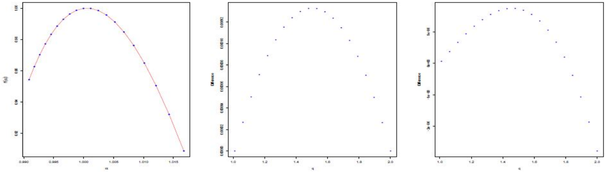

(a) $f(\alpha)$ versus α for large window

(b) Difference with linear function for large window

(c) Difference with Model 1 for large window

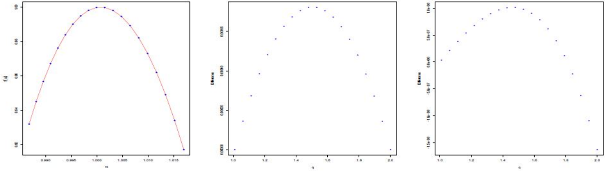

(d) $f(\alpha)$ versus α for small window

(e) Difference with linear function for small window

(f) Difference with Model 1 for small window

Figure: Analysis of large and small sky windows data

Computing the Rényi function for CMB data

Observation window	$[\alpha_{min}, \alpha_{max}]$	α_{max} - α_{min}	a	RMSE
Whole Sky	[0.9916, 1.0165]	0.024917	0.000513	$1.3602 \cdot 10^{-6}$
Large	[0.9908, 1.0167]	0.025846	0.000555	$1.3590 \cdot 10^{-6}$
Medium	[0.9893, 1.0159]	0.026620	0.000629	$1.1033 \cdot 10^{-6}$
Small	[0.9867, 1.0170]	0.030219	0.000745	$7.9095 \cdot 10^{-7}$
Very Small	[0.9842, 1.0543]	0.070150	0.001500	$1.3949 \cdot 10^{-5}$

Figure: Analysis of different sky windows data with Model 1

- For the log-normal model we present the results for all windows and for other models, only results for CMB data in a large window are given.
- For the log-normal model the simple linear regression approach was used whereas for the other models the non-linear regression approach was applied.
- The values of the parameter *a* and the root mean square error for deviations of Model 1 from the empirical Rényi function are given in the above table.
- The results also confirm that multifractality is very small as for all observation windows *a* is almost zero and $\alpha_{max} - \alpha_{min}$ is very small.

LA TROBE UNIVERSITY

Conclusions

- This study investigates the multifractal behaviour of spherical random fields and some applications to cosmological data from the mission Planck.
- The aim of this study is to introduce several multifractal models for random fields on a sphere and to propose simpler models where the Rényi function can be computed explicitly.
- All Rényi functions for the specified models exhibit either parabolic or approximately linear behaviours.
- We present the Rényi function computations for different CMB sky windows located at different places of the sphere.
- All the specified models fit to the actual CMB data.
- The analysis suggests that there may exist a very minor multifractality of the data.

Future Work

- Develop statistical tests for different types of Rényi functions;
- Prove that the theoretical results and the formulae for the Rényi functions are also valid for the values of q outside the interval $[1, 2]$;
- Study other models based on vector random fields (similar to Model 6), where the Rényi functions can be computed explicitly;
- Investigate changes of the Rényi functions depending on evolutions of random fields driven by Stochastic Partial Differential Equations(SPDEs) on the sphere;
- Apply the developed models and methodology to other spherical data, in particular, to new high-resolution CMB data from future CMB-S4 surveys.

LA TROBE UNIVERSITY

References

- Anh, V. Broadbridge, P. Olenko, A. & Wang, Y. (2018). On approximation for fractional stochastic partial differential equations on the sphere. Stochastic Environmental Research and Risk Assessment. 32:2585-2603.
- Broadbridge, P., Kolesnik, A. D., Leonenko, N., & Olenko, A. (2019). Random spherical hyperbolic diffusion. Journal of Statistical Physics, 177(5), 889-916.
- Harte, D. (2001). Multifractals: Theory and Applications. Chapman and Hall/CRC, Boca Raton
- Fryer, D. Olenko, A. Li, M. & Wang, Y. (2019). rcosmo: R Cosmic Microwave Background Data Analysis. R package version: 1.1.1.
- Fryer, D. Li, M. & Olenko, A. (2019). rcosmo: R Package for Analysis of Spherical, HEALPix and Cosmological Data, arXiv preprint arXiv:1907.05648.
- Leonenko, N., Nanayakkara, R., & Olenko, A. (2020). Analysis of Spherical Monofractal and Multifractal Random Fields with Cosmological Applications. arXiv preprint arXiv:2004.14522.
- Leonenko, N. & Shieh, N.-R. (2013). Rényi function for multifractal random fields. Fractals, 21(02), 1350009.
- NASA/IPAC INFRARED SCIENCE ARCHIVE. (2019). Retrieved September 11, 2019, from https://irsa.ipac.caltech.edu/data/Planck/release_2.

LA TROBE UNIVERSITY

Thank you